Pergamon

Geochimica et Cosmochimica Acta, Vol. 65, No. 12, pp. 2007–2016, 2001

0016-7037/01 $20.00 + .00

PII S0016-7037(00)00569-5

Geochemistry and petrology of Witwatersrand and Dwyka diamictites from South Africa: Search for an extraterrestrial component

HEINZ HUBER,[1] CHRISTIAN KOEBERL,[1,*] IAIN MCDONALD,[2] and WOLF UWE REIMOLD[3]

[1]Institute of Geochemistry, University of Vienna, Althanstrasse 14, A-1090 Vienna, Austria
[2]School of Earth and Environmental Sciences, University of Greenwich, Catham Maritime, Kent ME4 4AW, United Kingdom
[3]Impact Cratering Research Group, Department of Geology, University of the Witwatersrand, Johannesburg 2050, South Africa

(*Received November* 1, 2000; *accepted in revised form January* 18, 2001)

Abstract—Diamictites are poorly sorted sediments characteristically carrying coarse-grained clasts in a fine-grained matrix. They have generally been considered of glaciogenic or glaciomarine origin. Recently, however, it has been suggested that some massive tillite/diamictite layers could represent impact breccias. An earlier petrographic study of rock and mineral clasts from Dwyka Group diamictites revealed no evidence for shock metamorphism, such as planar deformation features. Detailed geochemical studies of diamictite samples from the Archean Witwatersrand Supergroup and the Dwyka Group of the Mesozoic Karoo Supergroup from South Africa are reported. We studied the contents of the siderophile elements in these breccias, as elevated abundances of such elements, especially iridium, could be indicative for an impact origin. By use of γ-γ coincidence spectrometry and other trace element analysis, geochemical tracers of extraterrestrial components were sought. However, no enrichments of indicator elements for extraterrestrial components, compared with ordinary continental crust, were found. Thus, neither geochemical nor petrographic evidence supports an impact origin of the diamictites from the Dwyka Group and the Witwatersrand Supergroup in South Africa. *Copyright © 2001 Elsevier Science Ltd*

1. INTRODUCTION

The term "diamictite" is defined as "A comprehensive, nongenetic term proposed by Flint et al. (1960) for a nonsorted or poorly sorted, noncalcareous, terrigenous sedimentary rock that contains a wide range of particle sizes, such as rock with sand and/or larger particles in a muddy matrix" (Bates and Jackson, 1987). Until recently, diamictites have been regarded only as a lithification product of glacial till, and therefore have often been termed "tillites" (e.g., Eyles and Eyles, 1983; Visser, 1994; von Brunn, 1994). Impact cratering is now widely accepted to be of fundamental importance for the evolution of all planetary bodies with a solid surface (e.g., Silver and Schultz, 1982; Melosh, 1989; Grieve, 1991; Dressler et al., 1994; French, 1998; Montanari and Koeberl, 2000). Texturally, impact ejecta may resemble tillites/diamictites; thus, various authors have suggested in recent years that some diamictite horizons could represent debris layers from catastrophic impact events. Oberbeck et al. (1993) and Rampino (1994) suggested that the massive Dwyka deposits of the Karoo Supergroup in South Africa (Fig. 1) could be remnants of ejecta layers from large impact events. These suggestions were based mainly on model calculations of thickness of globally deposited ejecta layers through extended bombardment of the Earth by extraterrestrial bodies. However, these authors could not obtain supporting evidence from characteristic shock deformation indicators, such as planar deformation features (PDFs), which only form as a result of the extreme pressure and strain rate conditions associated with hypervelocity impact (see, e.g., Stöffler, 1972; Stöffler and Langenhorst, 1994; Grieve et al., 1996; French, 1998; Montanari and Koeberl, 2000).

*Author to whom correspondence should be addressed (christian.koeberl@univie.ac.at).

Reimold et al. (1997) presented results of the first extensive search for PDFs or other shock microdeformation in some 75,000 rock and mineral clasts from Dwyka Group diamictites of the Karoo Supergroup in southern Africa. No evidence for shock metamorphism was observed in any of their samples.

To further investigate a possible origin for the South African Dwyka Group diamictites, we performed detailed geochemical analyses of a number of petrographically well-studied diamictite samples. If diamictites represent remnants of impact breccias, they could contain traces of the meteoritic projectile. In most cases, the contribution of meteoritic matter to impact melt and melt-bearing rocks or glasses is less than 1%, leading to only minimal chemical changes in the resulting impactites (e.g., Koeberl, 1998). Only elements of high abundance in meteorites, but low abundance in terrestrial crustal rocks, can be used to detect such a meteoritic component. Studies of the abundances and interelement ratios of the siderophile elements, such as Cr, Co, Ni, and especially the platinum group elements (PGEs), have been used for these investigations (see, e.g., Morgan et al., 1975; Palme et al., 1978; Palme, 1982). Addition of only 0.1% of a meteoritic (chondritic) component to a crustal rock would yield an enrichment of, for example, ~0.5 ppb iridium to the crustal abundance of ~0.02 ppb Ir in the resulting impact breccia (see Koeberl, 1998). Because of these low abundances, very sensitive analytical techniques, such as iridium coincidence spectrometry and inductively coupled plasma source mass spectrometry (ICP-MS), after chemical preseparation of the PGEs, must be applied.

In addition to an extensive suite of Dwyka Group diamictite samples, a number of samples from the Witwatersrand Basin, representing a diamictite horizon in the Government Subgroup of the Archean Witwatersrand Supergroup of South Africa, and, for comparison, an enigmatic sample of a breccia with clasts with confirmed shock metamorphic deformation (Rei-

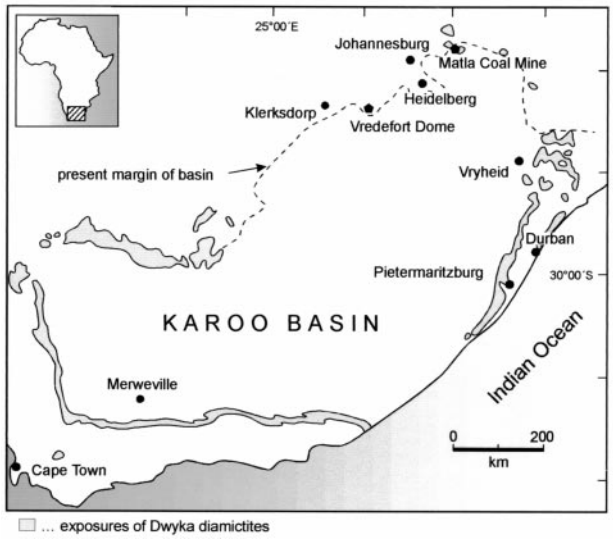

Fig. 1. Map of the Karoo Basin, with the Dwyka group diamictites in gray. Sample localities are the Umlaas Road Quarry east of Pietermaritzburg (UQ samples), Sjambokkraal near Merweville (V samples), Matla coal mine, Vredefort Dome, the East Rand basin in the Heidelberg area and the West Rand basin near Klerksdorp (Witwatersrand diamictites).

mold and Gibson, 1996), from the same stratigraphic interval in the Witwatersrand Supergroup, but from the collar of the Vredefort Dome, were analyzed.

2. EXPERIMENTAL

2.1. Samples

Twenty-three samples from different localities of the Late Carboniferous to Early Permian Dwyka Group of the Karoo Supergroup were chemically analyzed (Tables 1 and 2). Sixteen samples were collected at the Umlaas Road Quarry (UQ-1 to UQ-18) near Cato Ridge, east of Pietermaritzburg (Fig. 1); five samples (V1 to V5) from Sjambokkraal near Merweville were kindly provided by J. Visser (University of the Free State, Bloemfontein, South Africa), and two specimens (EGH 270 and MaCa1/2) were obtained from Matla Coal Mine in Mpumalanga Province, in the northeastern part of the Karoo Basin (Fig. 1). One possible diamictite from the western collar of the Vredefort Dome (K10E) was analyzed. Seven diamictites from the Coronation Formation of the Government Subgroup in the Witwatersrand Supergroup (SACS, 1980) were studied (samples HE-1, HE-2a/b and HE-3, RK12, RK20, WP87, 2627-72.40a and 2627-98.21a).

Several diamictite horizons have been described from the 2.9 to 2.71 Ga (Armstrong et al., 1991) Witwatersrand Supergroup (e.g., Stanistreet et al., 1988; Reynolds, 1991). In particular, so-called diamictites have been described from the Coronation Formation of the Lower Witwatersrand Supergroup, the Central Rand Group, and its equivalent formations in the West Rand goldfield near Klerksdorp (Fig. 1), the Bonanza/Welgegund Formations (SACS, 1980). Samples RK6 and RK12 represent the diamictite horizon in the Welgegund Formation, and RK20 and RK22 were sampled in the underlying Bonanza Formation of the West Rand goldfield area. These four samples were provided by W. E. L. Minter of the University of Cape Town. Three other diamictite samples (prefixed HE-) are derived from the Coronation Formation (specifically, a thin diamictite layer in the Coronation Shale Member) of the East Rand Basin. These samples were collected by T. S. McCarthy (University of the Witwatersrand) from surface exposures near Heidelberg town (Fig. 1), southeast of Johannesburg. The sampling site is located close to a location known as Fortuna's Siding.

Three samples for this study were obtained from boreholes on Farm Waterpoortje 281 in the western collar of the Vredefort Dome. The Dome represents the central uplift of the Vredefort impact structure (Reimold and Gibson, 1996; Gibson and Reimold, 1999), which, with an original diameter of 250 to ≥300 km (Therriault et al., 1997; Henkel and Reimold, 1998), involved the whole extent of the currently known Witwatersrand Basin. The Vredefort Dome and surrounding parts of the Witwatersrand Basin are known for the occurrences of abundant, often massive, pseudotachylitic breccias (e.g., Reimold and Colliston, 1994). A different type of breccia was identified in both Waterpoortje boreholes, occurring between 72.28- and 128.43-m depths. Mining geologists had classified these breccias as diamictite of the Coronation Shale Formation, the stratigraphic position of which had indeed been intersected in this interval. Samples WP87, 2627-72.40a, and 2627-98.21a originate from two boreholes (WP = Waterpoortje; 2627 = borehole 2627) on Waterpoortje 281, with the numerals indicating the sample depths.

Finally, sample K10E was also obtained in the western collar of the Vredefort Dome, from a surface exposure of what had been classified as Coronation Formation diamictite. However, Reimold and Gibson (1996) reported shock deformation in clasts from this material, which suggested that it was either shock metamorphosed Coronation diamictite or an injection of impact breccia into a favorable stratigraphic position—namely, the relatively soft Coronation shale.

2.2. Analytical Procedures

Major, minor, and trace elements were analyzed with X-ray fluorescence spectrometry (XRF) and instrumental neutron activation analysis (INAA). XRF analysis was performed at the University of the Witwatersrand, Johannesburg. For information on procedures, accuracy, and precision, see Reimold et al. (1994).

For INAA, rock samples were crushed manually in plastic wrap, then mechanically in an alumina (ceramic) jaw crusher, and then powdered with an automatic agate mill. Aliquots of ~150 mg were sealed into polyethylene vials. The sample vials were packed with well-characterized reference material into a larger polyethylene irradiation vial. The international granite standards AC-E and USGS. G-2 (Govindaraju, 1989), the Allende meteorite standard reference powder (Jarosewich et al., 1987), and—for Au and Ir—the mineralized gabbro PGE standard WMG-1 (CANMET 1994), were used as certified reference materials to determine the accuracy of the analysis.

The irradiation took place at the TRIGA Mark II type reactor at the Atominstitut der Österreichischen Universitäten in Vienna for 7 h at a flux of $\sim 2 \cdot 10^{12}$ n · cm^{-2} · s^{-1}. After a cooling period of 4 d, samples were transferred to the Institute of Geochemistry at the University of Vienna for further processing. First the sample vials were washed with HCl, NaOH, and hot water to remove any external contamination. To obtain reproducible measurement geometry, samples were centrifuged. All samples were counted repeatedly with an high-purity germanium detector with 1.8-keV resolution at 1332.5 keV and an efficiency of 48%. Further details on the methods (measuring times, instrumentation, precision, accuracy, etc.) are given in Koeberl (1993).

Because of the low iridium abundances encountered during INAA, the iridium content was additionally determined with the iridium coincidence spectrometry system at the Institute of Geochemistry at the University of Vienna. Seven crushed and powdered samples of ~50 mg each, as well as a series of the Allende meteorite reference sample (Jarosewich et al., 1987) that were diluted with high-purity quartz powder to produce standards with Ir concentrations between 35 ppt and 6.93 ppb, were sealed into high-purity quartz glass tubes. Samples and standards were packed into aluminum foil and an aluminum capsule, then irradiated for 48 h at the ASTRA reactor of the Forschungszentrum Seibersdorf, Austria, at a flux of $\sim 7 \cdot 10^{13}$ n · cm^{-2} · s^{-1}. After a cooling period of 10 weeks, the samples were first measured for 5 to 8 h. The samples that yielded results close to the detection limit were measured for at least another 24 h. Regression analysis was performed for the dilution series to provide good precision and accuracy. The calculated peak volumes were used to perform the unknown sample analysis with live time correction, decay time correction, flux correction, background subtraction, and comparison with the standards. For further details on this method (e.g., precision and accuracy), see Koeberl and Huber (2000).

Table 1. Major and trace element composition of Dwyka diamictites from the South African Karoo Basin.[a]

	Dwyka Group															
Element	UQ-2	UQ-3	UQ-5	UQ-6	UQ-7	UQ-9	UQ-10	UQ-11	UQ-12a	UQ-12b	UQ-13	UQ-14	UQ-15	UQ-16	UQ-17	UQ-18
SiO_2	66.7	66.4	70.6	66.3	66.4	66.4	66.3	66.8	81.9	66.5	67.2	68.0	67.5	68.8	68.5	67.9
TiO_2	0.67	0.66	0.67	0.73	0.70	0.74	0.74	0.73	0.62	0.76	0.72	0.64	0.76	0.77	0.74	0.71
Al_2O_3	13.1	13.4	12.7	13.7	13.6	13.9	13.8	13.8	7.54	13.8	13.8	13.1	13.4	13.5	13.2	13.1
Fe_2O_3	4.60	5.28	4.60	5.48	5.26	5.30	5.66	5.37	2.77	5.93	5.59	4.85	5.46	4.25	5.38	5.08
MnO	0.11	0.12	0.11	0.11	0.13	0.14	0.11	0.12	0.09	0.10	0.11	0.11	0.12	0.10	0.13	0.10
MgO	2.61	3.01	2.23	3.00	2.79	2.92	3.01	2.90	2.00	3.13	2.96	2.80	2.84	2.17	2.92	2.17
CaO	2.79	2.27	1.11	2.25	2.19	1.33	2.06	2.12	0.81	2.01	1.96	2.15	1.68	2.03	1.39	2.60
Na_2O	3.07	3.29	2.73	3.09	3.09	2.97	3.01	2.92	1.73	2.71	2.99	3.02	2.72	3.10	2.57	2.48
K_2O	2.36	2.32	3.01	2.44	2.66	2.79	2.52	2.51	0.98	2.52	2.30	2.50	2.47	3.25	2.11	3.08
P_2O_5	0.13	0.13	0.16	0.15	0.16	0.16	0.16	0.16	0.10	0.15	0.16	0.14	0.17	0.19	0.16	0.16
L.O.I.	3.17	2.82	2.06	2.44	2.43	2.64	2.52	2.42	1.38	2.29	2.06	2.29	2.72	1.72	2.67	2.38
Total	99.4	99.7	99.9	99.6	99.4	99.3	99.9	99.9	99.9	99.9	99.9	99.7	99.8	99.9	99.7	99.7
Sc	11.7	13.5	12.1	14.0	14.2	13.4	14.9	14.0	7.54	16.4	14.5	12.0	14.5	12.6	14.1	14.8
V	91	103	84	106	104	113	109	113	100	121	110	103	109	92	113	102
Cr	239	182	117	141	125	131	135	124	127	124	138	140	146	94.7	118	134
Co	14.1	16.6	11.8	16.1	14.9	15.7	16.6	14.9	9.65	17.4	16.2	14.1	16.3	9.62	15.0	15.5
Ni	53	76	41	49	51	57	72	46	59	60	47	37	65	30	26	60
Cu	7	10	14	16	9	10	13	13	2	23	11	6	7	35	5	19
Zn	66	76	72	69	77	77	78	84	38	117	90	50	86	66	85	99
Ga	16	150	46	100	69	49	32	63	16	150	102	10	38	11	99	81
As	1.86	1.83	3.21	1.85	2.59	1.24	1.87	2.27	3.56	1.75	2.42	1.93	3.36	4.97	4.31	2.28
Se	0.20	0.34	0.20	0.32	0.27	0.35	0.41	0.29	0.16	1.27	2.30	0.31	0.26	0.45	0.44	0.36
Br	0.30	0.20	1.02	1.04	1.02	0.25	0.51	1.37	0.51	1.74	1.36	0.74	0.73	0.38	1.06	0.98
Rb	100	88.8	107	89.3	96.8	94.1	92.9	95.0	36.1	97.6	107	84.0	95.6	122	93.1	143
Sr	164	174	141	176	172	134	177	173	74.0	173	160	167	142	144	130	167
Y	20	23	31	26	26	24	28	28	19	30	27	24	30	33	28	28
Zr	161	170	204	184	200	189	197	189	137	192	190	168	200	237	197	220
Nb	12	13	14	15	14	15	15	15	11	15	14	13	14	14	16	14
Sb	0.21	0.15	0.32	0.2	0.38	0.28	0.38	0.40	1.00	0.19	0.49	0.16	0.29	0.2	0.38	0.75
Cs	1.81	1.55	1.69	1.75	1.83	1.67	1.84	1.98	1.30	1.14	1.33	1.01	0.99	0.61	1.31	1.54
Ba	706	743	893	893	787	865	943	1031	541	878	955	729	892	917	803	819
La	29.9	32.4	37.7	36.2	37.3	34.3	39.6	37.9	22.6	40.5	40.3	31.9	37.3	31.7	36.8	42.7
Ce	57.9	62.4	79	70.1	76	67.7	77.4	71.9	44.0	76.1	79.1	60.5	81.6	65.4	73.9	86.5
Nd	24.4	31.1	36.6	31.8	30.9	33.2	35.9	38.1	19.8	33.9	35.3	27.1	36.8	32.6	33.1	39.8
Sm	4.63	5.17	6.83	5.69	5.57	5.27	6.10	6.79	3.90	6.32	6.23	4.68	6.91	6.52	5.87	6.90
Eu	1.08	1.11	1.37	1.23	1.25	1.18	1.36	1.27	0.87	1.49	1.37	1.15	1.47	1.36	1.31	1.36
Gd	4.85	4.42	6.0	5.67	6.51	4.93	6.82	5.57	2.95	5.80	6.18	4.12	5.92	5.03	5.13	5.99
Tb	0.61	0.66	0.98	0.81	0.95	0.69	0.92	0.82	0.49	0.84	0.86	0.63	0.88	0.95	0.80	0.92
Tm	0.30	0.31	0.39	0.33	0.32	0.33	0.42	0.38	0.28	0.38	0.39	0.31	0.45	0.44	0.37	0.42
Yb	2.06	2.36	3.01	2.52	2.39	2.21	2.84	2.80	2.01	2.82	2.79	2.16	3.04	3.01	2.55	2.99
Lu	0.31	0.36	0.45	0.37	0.35	0.37	0.41	0.41	0.30	0.42	0.41	0.31	0.41	0.44	0.37	0.43
Hf	3.99	4.67	6.19	5.17	5.71	5.11	5.89	5.30	3.80	5.47	5.85	4.59	5.69	7.28	5.91	5.69
Ta	1.04	0.93	0.85	0.88	1.02	0.97	1.01	0.82	0.51	1.02	0.92	0.71	1.11	0.60	1.16	0.90
W	1.84	3.20	0.70	1.36	0.70	1.82	0.90	0.10	1.74	0.10	1.72	1.75	1.26	0.43	1.21	1.14
Ir (ppb)	<1	<2	<2	<2	<1	<3	<2	<2	<1	<2	<2	<2	<3	<1	<2	<2
Au (ppb)	2	8	5	2	6	5	6	4	5	1	4	6	7	1	5	5
Th	11.8	12.4	12.9	13.0	14.1	13.5	13.6	14.5	6.98	13.6	14.1	10.9	14.5	9.12	13.7	13.6
U	2.38	1.75	2.56	1.82	2.22	2.21	2.48	2.53	1.70	2.41	2.19	1.75	1.20	2.27	1.65	2.98
K/U	8276	11024	9798	11163	10001	10510	8474	8254	4787	8721	8748	11886	17132	11929	10680	8617
Th/U	4.96	7.09	5.04	7.14	6.35	6.11	5.48	5.73	4.11	5.64	6.44	6.23	12.1	4.02	8.30	4.56
La/Th	2.53	2.61	2.92	2.78	2.65	2.54	2.91	2.61	3.24	2.98	2.86	2.93	2.57	3.48	2.69	3.14
Zr/Hf	40.4	36.4	33.0	35.6	35.0	37.0	33.4	35.7	36.1	35.1	32.5	36.6	35.1	32.6	33.3	38.7
Hf/Ta	3.84	5.02	7.28	5.88	5.60	5.27	5.83	6.46	7.45	5.36	6.36	6.46	5.13	12.1	5.09	6.32
La/Yb	9.81	9.28	8.46	9.71	10.5	10.5	9.42	9.15	7.60	9.70	9.76	9.98	8.29	7.12	9.75	9.65
Eu/Eu*	0.70	0.71	0.66	0.66	0.63	0.71	0.64	0.63	0.78	0.75	0.67	0.80	0.70	0.73	0.73	0.65

[a] Major elements (wt%). L.O.I., loss on ignition at 1100°C. All Fe as Fe_2O_3, trace elements (ppm), except as noted.

Concentrations of the noble metals iridium, ruthenium, rhodium, platinum, palladium, and gold were determined by a Ni sulfide fire assay with Te coprecipitation and ICP-MS procedure. This method was modified from Jackson et al. (1990) to accommodate a small sample mass (typically 7–14 g), enhance detection limits, and minimize the reagent blank. Typically, 6 g of Na-carbonate, 12 g borax, 0.9 g sulfur, 1.08 g carbonyl-purified Ni, and 3.5 g of silica were required for fusion of a 10-g sample aliquot. Masses of sulfur and Ni were fixed, but masses of the other reagents were proportionally increased or decreased to accommodate larger or smaller samples. The reagents were thoroughly mixed and transferred into a fire-clay crucible before being fired for 90 min at 1000°C. The buttons were dissolved in concentrated HCl,

Table 2. Major and trace element composition of various diamictites from South Africa.[a]

	Dwyka Group							Vredefort	Witwatersrand							
Element	V-1	V-2	V-3	V-4	V-5	EGH 270	MaCa 1/2	K10E	HE-1	HE-2a/b	HE-3	RK 12	RK 20	WP 87	2627-72-40a	2627-98-21a
SiO_2	68.2	69.0	70.6	68.2	71.3	70.4	61.4	79.9	67.4	71.0	71.3	90.7	83.4	67.5	74.4	79.3
TiO_2	0.69	0.69	0.66	0.68	0.64	0.89	0.60	0.42	0.54	0.57	0.41	0.14	0.18	0.28	0.22	0.21
Al_2O_3	12.9	13.1	12.8	13.0	12.3	12.6	8.13	8.66	14.1	11.3	9.23	2.50	7.94	13.2	12.5	10.5
Fe_2O_3	5.05	5.09	4.50	5.25	4.49	5.51	12.2	4.80	8.08	10.0	5.55	3.02	2.32	8.45	3.52	3.35
MnO	0.13	0.13	0.10	0.15	0.11	0.10	0.20	0.06	0.04	0.07	0.10	0.03	0.03	0.11	0.07	0.04
MgO	2.42	2.45	2.16	2.46	2.06	0.54	1.62	1.40	0.27	2.26	5.07	0.58	0.88	3.72	1.50	1.38
CaO	2.01	1.41	1.38	1.30	1.05	0.78	2.16	0.61	0.03	0.04	3.70	0.11	0.23	0.78	1.65	0.57
Na_2O	2.66	2.76	2.68	2.86	2.60	0.17	0.45	0.63	0.19	0.08	0.36	0.04	0.09	1.05	2.31	1.07
K_2O	2.89	2.73	2.91	2.68	2.68	0.96	1.95	1.96	1.97	1.88	0.81	0.45	2.06	2.61	2.19	2.04
P_2O_5	0.17	0.16	0.16	0.15	0.15	0.11	0.16	0.04	0.02	0.05	0.10	0.03	0.04	0.11	0.05	0.04
L.O.I.	2.77	2.26	2.04	2.61	1.98	7.81	10.32	1.28	6.67	2.50	3.01	0.92	1.66	2.16	0.78	1.46
Total	99.9	99.8	99.9	99.3	99.3	99.9	99.2	99.8	99.2	99.7	99.7	98.5	98.8	99.9	99.1	99.9
Sc	12.8	13.0	11.6	13.1	11.8	12.1	8.54	6.39	12.8	10.7	15.2	2.32	5.31	14.5	8.61	7.61
V	99.0	92.0	82.0	91.0	75.0	148	93.0	56.0	100	101	107	32	52	122	84	69
Cr	121	119	124	175	97.4	173	122	275	778	394	566	192	293	935	369	354
Co	14.1	13.5	11.3	14.9	11.9	7.79	13.8	14.1	4.97	5.87	27.5	9.20	12.9	42.1	18.4	18.0
Ni	58	65	32	59	35	25	39	75	122	114	171	24	49	275	105	68
Cu	3	7	6	13	6	7	6	13	26	5	9	111	90	109	81	84
Zn	76	75	81	82	77	69	45	43	33	43	47	85	69	132	109	116
Ga	19	41	63	41	3	17	56	5	31	19	14	10	11	76	12	15
As	3.15	3.89	3.56	2.69	3.17	12.7	9.68	0.28	15.3	7.56	13.2	16.9	15.8	9.40	13.3	11.0
Se	0.45	0.36	0.33	0.34	0.30	0.30	0.33	0.10	0.01	0.28	0.07	0.09	0.20	0.12	0.15	0.22
Br	0.29	1.05	0.24	0.17	0.94	0.50	0.38	0.56	1.9	0.1	<0.1	1.4	1.2	1.5	1.0	0.8
Rb	119	111	103	93.5	106	34.6	111	66.2	85.2	84.7	12.8	12.2	71.5	93.8	114	83.1
Sr	145	138	146	144	135	113	54.0	107	72.0	75.0	261	7.0	20.0	160	218	108
Y	30	29	30	27	29	42	27	8	14	14	8	5	8	22	15	16
Zr	219	197	204	187	197	362	256	115	178	131	68.0	121	241	228	253	271
Nb	15	14	14	14	14	18	14	8	11	10	6	5	8	10	10	9
Sb	0.23	0.27	0.33	0.15	0.10	1.58	0.78	0.54	0.89	1.18	0.79	3.30	0.90	0.90	0.90	0.80
Cs	2.37	2.22	1.62	1.64	1.65	1.08	1.55	5.47	2.24	1.92	0.54	0.73	2.59	9.40	11.4	5.10
Ba	845	802	895	847	856	351	286	323	471	302	129	85	411	466	461	559
La	42.5	37.8	38.2	38.3	35.7	54.3	29.0	21.6	5.35	21.0	7.52	10.1	16.1	25.8	30.5	31.5
Ce	87.0	77.0	74.6	75.4	76.5	110	55.4	41.3	8.31	34.3	15.3	20.2	34.1	49	53.8	56.8
Nd	38.1	36.7	35.3	35.2	34.7	55.6	25.6	14.3	5.34	15.7	9.01	8.64	14.7	22.1	21.4	22.9
Sm	7.14	6.48	7.16	6.31	6.34	9.00	4.45	2.27	1.52	2.53	1.18	1.66	2.73	4.41	3.79	3.96
Eu	1.42	1.35	1.37	1.30	1.32	1.83	1.09	0.67	0.49	0.75	0.42	0.35	0.40	1.20	1.35	1.15
Gd	6.05	6.17	5.73	4.61	6.58	5.83	6.23	1.60	1.32	1.60	0.92	1.23	2.11	4.35	3.15	3.24
Tb	0.91	0.88	0.89	0.82	0.81	0.99	0.76	0.22	0.25	0.29	0.14	0.19	0.32	0.74	0.52	0.5
Tm	0.43	0.41	0.44	0.35	0.36	0.46	0.45	0.12	0.21	0.21	0.09	0.11	0.16	0.41	0.26	0.25
Yb	2.99	3.03	3.16	2.74	2.92	4.38	3.36	0.82	1.64	1.46	0.77	0.78	1.05	2.68	1.76	1.64
Lu	0.45	0.45	0.44	0.41	0.43	0.67	0.51	0.14	0.27	0.23	0.14	0.12	0.13	0.38	0.24	0.26
Hf	6.14	5.51	6.39	6.04	6.43	8.94	7.51	3.72	4.44	3.71	1.94	2.96	6.39	6.24	6.46	7.01
Ta	0.62	0.82	0.94	0.83	0.90	0.77	0.95	0.33	0.50	0.50	0.26	0.28	0.65	0.77	0.69	0.64
W	1.21	2.87	0.71	1.81	0.52	1.47	0.27	0.36	0.16	1.43	1.15	0.67	0.17	21.8	0.58	<1.2
Ir (ppb)	<3	<3	<2	<1	<1	<2	<2	<2	<2	<2	<3	<2	<3	<2	<1	<3
Au (ppb)	1	2	6	7	6	1	4	8	3	3	4	8	3	2	3	6
Th	13.8	12.6	12.1	12.7	12.5	11.9	11.2	4.63	5.97	4.25	1.61	2.49	6.78	5.99	8.25	6.45
U	2.81	2.51	2.75	2.40	2.36	2.90	2.12	1.75	2.59	1.67	0.64	3.77	5.73	3.68	5.11	3.31
K/U	8556	9060	8808	9296	9453	2759	7664	9346	6336	9390	10483	995	2996	5910	3571	5136
Th/U	4.91	5.02	4.40	5.29	5.30	4.10	5.28	2.65	2.31	2.54	2.52	0.66	1.18	1.63	1.61	1.95
La/Th	3.08	3.00	3.16	3.02	2.86	4.56	2.59	4.67	0.90	4.94	4.67	4.06	2.37	4.31	3.70	4.88
Zr/Hf	35.7	35.8	31.9	31.0	30.6	40.5	34.1	30.9	40.1	35.3	35.1	40.9	37.7	36.5	39.2	38.7
Hf/Ta	9.90	6.72	6.80	7.28	7.14	11.6	7.91	11.3	8.88	7.42	7.46	10.6	9.83	8.10	9.36	11.0
La/Yb	9.61	8.43	8.17	9.45	8.26	8.38	5.83	17.8	2.20	9.72	6.60	8.75	10.4	6.51	11.7	13.0
Eu/Eu*	0.66	0.65	0.65	0.74	0.62	0.77	0.63	1.07	1.06	1.14	1.23	0.75	0.51	0.84	1.19	0.98

[a] Major elements (wt%), L.O.I., loss on ignition at 1100°C. All Fe as Fe_2O_3, trace elements (ppm), except as noted.

and noble metals that had entered the solution were coprecipitated with Te with $SnCl_2$ as a reductant. Finally, soluble PGE chloro-complex solutions were spiked with Cd and Tl as internal standard monitors for instrumental drift, and noble metal concentrations were determined by external calibration on a VG Elemental PQ2$^+$ Plasmaquad ICP-MS by use of procedures similar to those outlined above. The accuracy of the analysis was determined by analysis of the reference materials Peridotite-WPR1 (CANMET, 1994) and Komatiite-Wits1 (Tredoux and McDonald, 1996). For details of the method, including detection limits and typical reagent blanks, see Koeberl et al. (2000) and Huber et al. (2000).

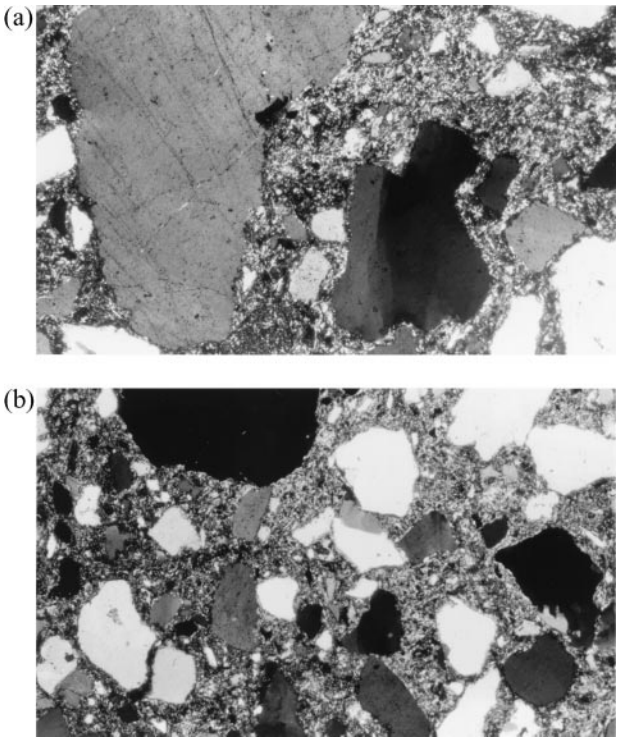

Fig. 2. Microphotographs of Witwatersrand diamictites. (a) Sample RK6, with typical textural appearance; irregular fluid inclusion trails and undulatory extinction are the only microdeformation effects observed; 2.2 mm wide, crossed nicols. (b) Sample RK12. This breccia is matrix dominated and clasts are of much more restricted and smaller grain sizes than in RK6; 3.5 mm wide, crossed nicols.

3. RESULTS

3.1. Petrography: Dwyka Group Diamictites

Typical Dwyka diamictite samples comprise generally well-rounded, but locally angular to subrounded, mineral and lithic clasts in a fine-grained, clastic matrix rich in phyllosilicate minerals. The matrix also contains a large component of extremely fine-grained mineral fragments, mostly of quartz and some feldspar. The clast populations of Dwyka diamictites are varied for samples from different parts of the Dwyka Group in the Karoo Basin (Reimold et al., 1997) and comprise a range of different precursor rock types, including varied igneous, metamorphic, and metasedimentary lithologies. Details on the mineralogical variations of this sample suite are provided in Reimold et al. (1997). As discussed by these authors, no evidence of shock deformation was observed in thin sections of a large number of Dwyka Group samples, including all those samples that are subject to the present geochemical investigation.

3.2. Witwatersrand Diamictites

3.2.1. West Rand Samples

Four samples of Government Subgroup diamictite from the West Rand region of the Witwatersrand Basin were analyzed. Sample RK6 (Fig. 2a) has 40 vol% of phyllosilicate-rich matrix and a sediment-dominated population of angular to subrounded clasts. The main clast type is quartz, with some minor chert, and <1 vol% of granite-derived and dolomite clasts, respectively. Grain sizes vary from 3 mm to <50 μm.

Sample RK12 is quite different from RK6; it is matrix dominated (~75 vol%), and has a bimodal clast size distribution, with maxima at 3 to 6 mm and ~0.5 mm. Both well-rounded (including most of the large clasts), and angular and subangular varieties occur in both grain-size ranges. The clast population is dominated by quartz and quartzite fragments, with 5 to 10 vol% chert and minor pyrite. In comparison with RK6, the matrix of RK12 (Fig. 2b) is less argillaceous than that of RK6.

Sample RK20, although from a different stratigraphic horizon, resembles RK6 but is characterized by a somewhat wider grain size distribution (up to 7 mm). Phyllosilicate-rich matrix makes up 45 vol% of this breccia. The population of well-rounded to angular clasts (this sample has more rounded clasts than RK6) is similar to that of RK6. Sample RK22, at 30 vol% matrix, appears intermediate between RK6 and RK12. Here, up to 15 vol% of mostly rounded chert clasts occur. Oherwise, the clast population is similar to that of the other RK samples.

No significant microdeformation was observed in any of these samples. Deformation is limited to rare undulatory extinction and irregular fluid inclusion trails in quartz. Intragranular fracturing is also rare, and only a few near-planar fluid inclusion trails were observed. These are much wider (>10 μm) than shock metamorphic PDFs and are irregularly spaced.

The diamictite samples from the East Rand have the following petrographic characteristics. Sample HE-1 is composed of >50 vol% goethite-rich mylonitic matrix and a clast population dominated by quartz and quartzite, with ~5 vol% of chert, <5 vol% of K-feldspar, and other, presumably granitoid- or vein quartz–derived, fragments, plus ~2 vol% of shale particles. The ductile deformation of this rock, which occurred after solidification of the breccia, was accompanied by cataclasis. Although most clasts are well rounded, angular forms occur as well. On thin-section scale, the largest clasts in these samples are 2 to 3 mm in size.

Sample HE-2a/b is even more matrix rich (55 vol%) than the HE-1 specimen. Quartz and quartzite clasts are dominant, besides ~7 vol% chert and minor biotite, schist, and carbonate. Granitoid-derived clasts (including the biotite clasts) may total 5 vol%. Clasts are <3 mm in size and subrounded to rounded. This sample has also suffered ductile deformation, as evidenced by a slight parallel alignment of clasts. HE-3 is different from all other studied Witwatersrand diamictite samples. The content of phyllosilicate matrix is comparatively very low (25 vol%), and the clast population contains a large component of generally well-rounded schist and shale clasts (representing the majority of the large grains between 2 and >5 mm). These clasts account for ~35 vol%. Chert (~10 vol%) and some feldspar and biotite clasts complete the clast population.

Microdeformation in sample HE-1 is stronger than in all other Witwatersrand diamictite samples, but again, no characteristic shock deformation was found. Many quartz clasts display undulatory extinction believed to be the result of post-depositional tectonic overprint. The other East Rand samples display some undulatory extinction and fluid inclusion trails in a few clasts. Overall, the Witwatersrand diamictite samples do not display any indication of shock metamorphic deformation

and are rather varied with regard to both microtextural and clast population characteristics.

3.2.2. Diamictite from the Waterpoortje Borehole of the Vredefort Dome

Near the geographic center of the Witwatersrand Basin is the location of the Vredefort Dome, the origin of which as the result of either the impact of a large extraterrestrial bolide or of an endogenic catastrophe has long been controversial (e.g., Reimold and Gibson, 1996; Gibson and Reimold, 1999). However, unequivocal evidence in favor of an impact origin has recently been obtained: Leroux et al. (1994) demonstrated that planar microdeformation features in quartz of Vredefort rocks represent basal twin lamellae, which, as deformation features, have only been described from impact-deformed rocks. Kamo et al. (1996) identified shock-metamorphosed zircons with planar microdeformation structures and granular shock texture in rocks from Vredefort and determined a well-constrained single zircon U-Pb age of 2023 $\pm$ 4 Ma for the impact event. Finally, Koeberl et al. (1996) used Re-Os isotope studies to identify a minor meteoritic component in melt rock dykes of Vredefort Granophyre, confirming that this enigmatic melt rock represents impact melt breccia.

Drillcore into Government Subgroup strata from farm Waterpoortje 281 in the western sector of the upturned supracrustal rocks of the collar of the Vredefort Dome contains an interval of fine to very coarse-grained diamictite. This material contains abundant shock metamorphosed quartz clasts, with planar fluid inclusion trails that represent annealed PDFs, as well as some diaplectic quartz glass. A suite of samples was made available for petrographic analysis. The whole interval is rather heterogeneous. Sections with predominantly angular clasts alternate with others that carry only rounded to subrounded clasts. In general, the matrix is sericite dominated and comprises ~30 to 40 vol% of the samples. The clast population is dominated by quartz and quartzite particles. Minor chert was noted, and granitoid-derived plagioclase, K-feldspar (orthoclase and microcline), and biotite occur in individual samples at significant amounts. A sample from a depth of 98.21 m shows discernible alignment of clasts and a slight mylonitic fabric in the matrix. Clast sizes are highly variable from sample to sample, and individual clasts may reach sizes of 1 cm or more. Many quartz grains contain several sets of planar fluid inclusion trails (Figs. 3a,b), which are narrowly spaced and are classified as decorated PDFs of the Vredefort type (e.g., Leroux et al., 1994; Reimold and Gibson, 1996). Incipient annealing is observed along some PDFs. Several of our samples are cut by <0.5-cm-wide veinlets of clast-rich pseudotachylitic breccia (Fig. 3c), the matrix of which exhibits clear evidence of melting (e.g., in the form of feldspar microlites; small quartz clasts in such matrix are often of amoebic shapes, which may indicate marginal resorption by melt). Contacts between large (several centimeters wide) quartzite clasts and such melt rock indicate a violent emplacement of the breccia, which led to slices of quartzite being sheared off the contact wall.

These results are clear evidence of shock metamorphism and lead to the question that either this interval represents impact-affected Archean Witwatersrand diamictite or an injection of fragmental impact breccia. The fact that narrow veinlets of pseudotachylitic breccia transect this horizon cannot be utilized to solve this problem. Cross-cutting relationships between fragmental impact breccia and such melt breccia could have been formed at different times during the catastrophic formation of the impact structure.

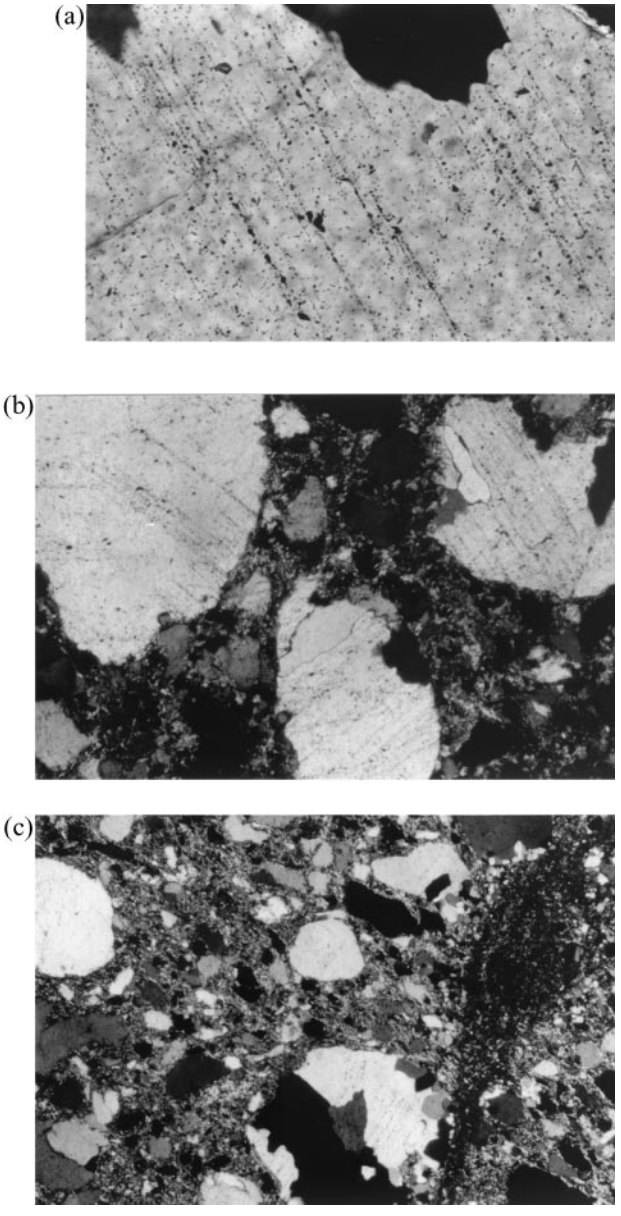

Fig. 3. Microphotographs of "diamictite" from the Vredefort Dome Waterpoortje boreholes. (a) Sample from a depth of 98.21 m; quartz grain with planar fluid inclusion trails; width of field of view, 1.1 mm, crossed nicols. (b) Three quartzite clasts with PDFs; note that the clast in the upper left has two sets of microdeformations of different orientations; also note that the clasts at the upper right has been partially annealed and that the microdeformations have been affected by this annealing process; this effect can also be seen in Figure 4a; from a depth of 72.40 m, 1.1 mm wide, crossed nicols. (c) This sample, from a 125.10-m depth, is transected by a narrow veinlet of pseudotachylitic breccia (this term is used because it is not clear whether this material represents ultraclastic or a melt breccia; cf. Reimold, 1995, for discussion of terminology). Note the considerable variety in grain sizes and the overall rounded appearance of clasts.

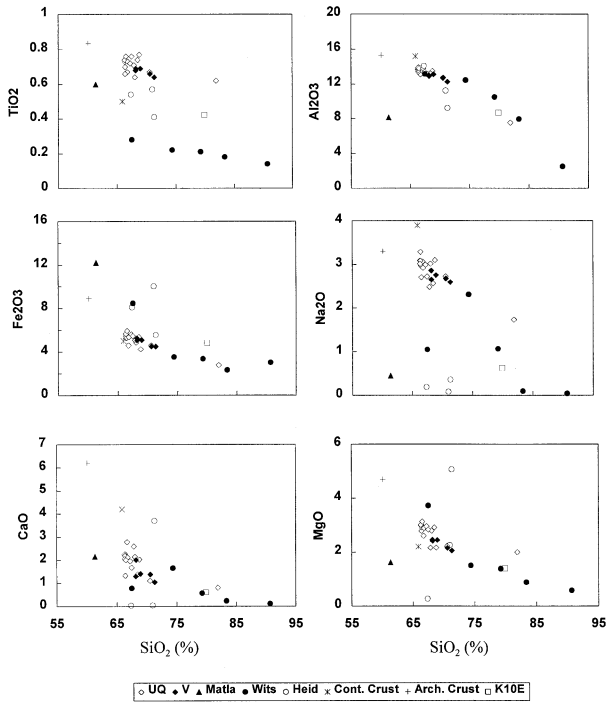

Fig. 4. Harker diagrams of Dwyka diamictites and diamictite samples from the Witwatersrand compared with a sample from the Vredefort dome and two specimens from the Matla coalmine. The sample K10E from Vredefort is similar to all other samples from the Witwatersrand, except in the content of TiO_2.

In the absence of structural clues to the nature of the breccia horizon, the textural appearance of the quartz/quartzite clast-dominated breccia and clast population data may provide further insight. The dominance of rounded over angular clasts in most samples suggests a sedimentary origin rather than violent disruption of precursor material to fragmental impact breccia. However, at this stage, it is not possible to fully resolve the origin of this enigmatic breccia. Further studies of other drill-cores from the collar and wider environs of the Vredefort Dome, as well as detailed sampling and analysis of this material is required.

3.3. Bulk Composition

The contents of 36 major and trace elements were determined in all samples by INAA. In addition, the major elements Si, Ti, Al, Fe, Mn, Mg, Ca, Na, K, and P and the trace elements Y, Nb, V, and Cu were analyzed by XRF. All analytical results are listed in Tables 1 and 2. The abundances of Fe (all Fe as Fe_2O_3), Ni, Sr, Ba, and Zr were calculated as the average of the XRF and INAA results. In Figure 4, the major element abundances for the samples analyzed in this study are plotted against SiO_2 contents. The compositions of average continental and average Archean crust (data from Taylor and McLennan, 1985) are also plotted. Dwyka samples from the Umlaas Road Quarry, with one highly siliceous exception, and from the Western Cape locality plot, respectively, into relatively tight clusters; in comparison, Dwyka samples from Matla have a very different composition. This is in agreement with the variable clast populations observed for each sample location. However, all samples from one specific locality have very similar clast populations.

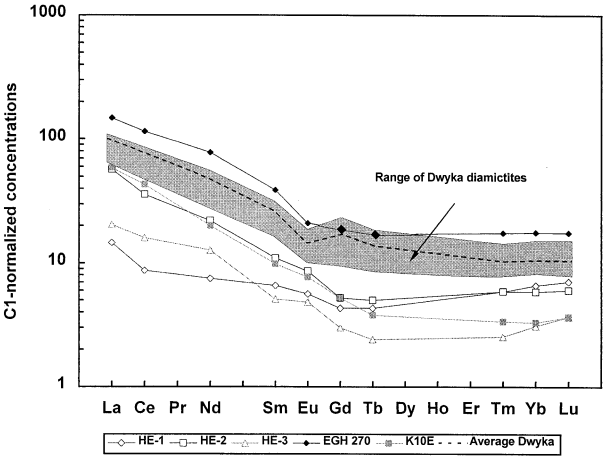

Fig. 5. Chondrite-normalized REE patterns (normalization factors by Taylor and McLennan, 1985). Elements were analyzed with INAA. The curves represent typical crustal rock abundances patterns; only slight differences can be seen between the Dwyka Group diamictites and the Wits Government Supergroup diamictites (sample HE-1 to HE-3) and sample K10E from the Vredefort Dome.

The Witwatersrand West Rand and Heidelberg diamictite samples have variable compositions, again in keeping with their respective clast populations. Clearly different sources must have contributed to this widespread but stratigraphically very well defined Coronation Formation diamictite. The values for average continental crust plot relatively close to those for the Dwyka samples but do not relate to the composition of the Witwatersrand diamictites. Average Archean crust is depleted in SiO_2 in comparison to all samples analyzed. The enigmatic sample K10E from the Vredefort Dome generally plots into the range defined by the Government Subgroup samples, but it is somewhat enriched with regard to TiO_2, comparable to Heidelberg sample HE-3.

The chondrite-normalized rare earth element (REE) patterns (normalization factors after Taylor and McLennan, 1985) are shown in Figure 5. All patterns for Dwyka Group diamictites are similar. Especially the samples from the Umlaas Road Quarry and those from Merweville show similar element distributions with a slight negative europium anomaly ($Eu/Eu^* \approx 0.75$). Decreased abundances of Al, Fe, and a lower loss on ignition, as well as a distinct depletion in REE abundances according to the somewhat more quartzose composition (82% SiO_2), characterize sample UQ-12a.

UQ-16 and EGH 270 from Matla Coal Mine show a higher Hf/Ta ratio of ~12 compared with the average of ~5 to 7. The La/Th ratios scatter around 2.8, with exceptions being EGH 270 from Matla, the Vredefort sample K10E, and the Heidelberg samples HE-2 and HE-3 with values of ~4.6, and HE-1 with an La/Th ratio of 0.9. The La_N/Yb_N ratios generally range from 8 to 10; only UQ-12a and UQ-16 show flatter REE patterns.

The diamictite samples from the East Rand basin south of the town of Heidelberg (samples HE-1 to HE-3) show a distinct chemical composition. They are generally depleted in REE

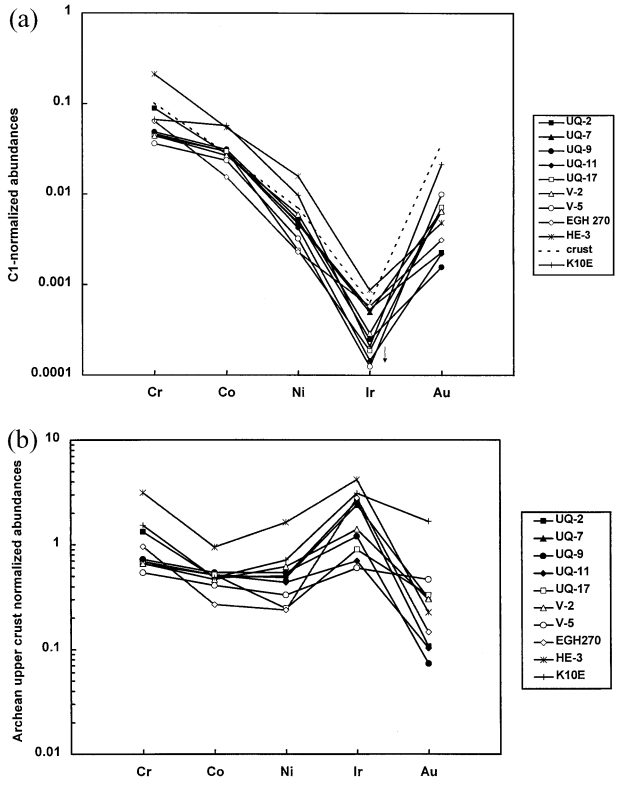

Fig. 6. Normalized siderophile element concentration patterns. Elements analyzed by INAA. No enrichment in Ni or Ir, which would be indicative of an impact-related rock, can be seen. (a) Data normalized to C1 chondritic (Orgueil) abundances (data from Palme et al., 1981). (b) Data normalized to Archean upper crust (data from Taylor and McLennan, 1985).

contents, and have a positive slope for the HREE (heavy rare eastly elements) pattern and a positive europium anomaly (Eu/Eu* $\approx$ 1.1). In addition, these samples are highly enriched in Cr and Ni, compared to the Dwyka diamictites. The samples from the Bonanza and Welgegund Formation show considerable variations in composition. Sample 2627.72.40a from the Waterpoortje borehole has a composition similar to that of the samples from Heidelberg. The other specimens from the Coronation Formation diamictite have concentrations within the range of the Dwyka samples. Sample K10E, from the western collar of the Vredefort Dome, seems to be intermediate between the Dwyka samples and the Government Subgroup samples. Although generally depleted in REE and having a positive europium anomaly, this sample shows a negatively sloping HREE pattern.

For the comparison of siderophile element concentration patterns (Fig. 6), the values obtained by INAA were used. Generally, the abundances are in the range of 0.1 to 0.001 chondritic. The pattern normalized to Orgueil C1 carbonaceous chondrite values (Fig. 6a) shows no significant enrichment in siderophile elements but a distinct depletion in the contents of Ni or Ir, compared with average continental crustal concentrations. Sample K10E shows increased abundances in Co and Ni; the other siderophile abundances are within the range of the Dwyka diamictite samples. When normalized to Archean upper crust (Fig. 6b), a distinct depletion of Au can be seen for all samples. The other siderophile elements lie within a factor of two of the Archean upper crust values. The abundances of iridium and gold (INAA values) do not show any distinct trend, partly because the Ir abundances were below the detection limit for all samples.

Table 3. Comparison of iridium concentrations in South African diamictites from the Karoo Basin determined by INAA, ICS, and ICP-MS (concentrations, ppb).[a]

Sample	INAA	ICS	ICP-MS
UQ-2	1.0	0.093 ± 0.019	0.26 ± 0.04
UQ-7	<1.0	0.070 ± 0.016	0.24 ± 0.05
UQ-16	0.8	0.515 ± 0.044	—
UQ-17	<2.1	0.086 ± 0.018	0.09 ± 0.01
EGH270	<2.1	0.373 ± 0.048	0.28 ± 0.08
HE-1	<2.2	0.209 ± 0.048	—
HE-3	<2.7	0.512 ± 0.060	0.42 ± 0.07

[a] INAA, instrumental neutron activation analysis; ICS, iridium coincidence spectrometry; ICP-MS, noble metal analysis by NiS fire assay with Te coprecipitation and ICP-MS procedure.

3.4. Platinum Metal Group Elements

The sensitive coincidence measurements of the iridium contents were performed for those samples that showed an indication of elevated iridium abundance from the INAA data. The results for the UQ-2, UQ-7, UQ-16, UQ-17, and EGH 270 Dwyka samples, as well as for two samples of Witwatersrand diamictite (HE-1 and HE-3) are presented in Table 3. Values are calculated as counts ± 1.96 times the square root of the counts for a 95% confidence interval. The high iridium contents of the samples UQ-2 and UQ-16 are intriguing but do not allow any unambiguous conclusions regarding their cause. When we compare the results of the different Ir determination methods in this study, we find a good correlation between the iridium coincidence spectrometry and ICP-MS data for the samples UQ-17, EGH 270, and HE-3. The respective data for UQ-2 show some differences, and the discrepancy is relatively large for UQ-7. These variations could result from sample heterogeneity (cf. McDonald, 1998; Pearson and Woodland, 1999).

Five samples from the Umlaas Road Quarry, two from other Dwyka localities, and one each from Vredefort (K10E) and the Heidelberg area were analyzed with ICP-MS. The results are shown in Table 4. The highest gold content of 5 ppb was found for the Vredefort sample. The Dwyka samples and Witwatersrand diamictites have lower abundances of 0.2 to 1.4 ppb. For Ir, the values show a wide range, but it is possible to define two groups. The Ir concentrations are between 0.07 and 0.28 ppb for the Umlaas Road Quarry and Matla Coal Mine Dwyka diamictites. The Vredefort and Heidelberg samples contain slightly more Ir, up to 0.42 ppb for the HE-3 sample. The values for other PGEs (Ru, Pt, Rh and Pd) are very similar for all samples.

Normalizing these data to C1, E4, H5, and L6 meteorite abundances (similar to the procedure discussed in Koeberl et al., 2000) does not yield chondritic PGE abundance patterns. Figure 7 shows the Orgueil C1 normalization diagram obtained the normalizing factors of Palme et al. (1978; 480 ppb Ir, 690 ppb Ru, 130 ppb Rh, 1050 ppb Pt, 530 ppb Pd, and 140 ppb

Table 4. Platinum group element abundances analyzed with ICP-MS (concentrations, ppb).

Sample	IR	Ru	Rh	Pt	Pd	Au
UQ-2	0.26 ± 0.04	0.27 ± 0.03	0.09 ± 0.01	0.73 ± 0.23	0.98 ± 0.28	0.32 ± 0.06
UQ-7	0.24 ± 0.05	0.38 ± 0.08	0.10 ± 0.02	1.20 ± 0.10	1.50 ± 0.20	0.93 ± 0.15
UQ-9	0.12 ± 0.02	0.16 ± 0.02	0.09 ± 0.02	0.93 ± 0.15	1.30 ± 0.10	0.22 ± 0.10
UQ-11	0.07 ± 0.02	0.10 ± 0.03	0.06 ± 0.03	0.73 ± 0.04	0.96 ± 0.08	0.31 ± 0.10
UQ-17	0.09 ± 0.01	<0.1	0.06 ± 0.01	0.54 ± 0.11	0.79 ± 0.10	1.00 ± 0.30
V-2	0.14 ± 0.02	<0.1	0.06 ± 0.02	0.68 ± 0.12	0.83 ± 0.20	0.91 ± 0.21
V-5	0.05 ± 0.01	<0.1	0.08 ± 0.02	0.57 ± 0.13	0.78 ± 0.06	1.40 ± 0.60
EGH270	0.28 ± 0.08	0.32 ± 0.07	0.10 ± 0.02	1.20 ± 0.20	0.81 ± 0.20	0.44 ± 0.03
HE-3	0.42 ± 0.07	1.10 ± 0.10	0.48 ± 0.03	3.10 ± 0.10	4.60 ± 0.20	0.68 ± 0.02
K10E	0.31 ± 0.04	0.47 ± 0.10	0.10 ± 0.01	0.98 ± 0.18	1.10 ± 0.30	5.00 ± 0.50

Au). The normalized PGE patterns are similar for most of the Dwyka samples, with an increase in slope from Ir to Au but with no significant differences between samples. Only one sample of Government Subgroup diamictite (HE-3) shows a slight enrichment of all PGE (although not Au), but this signature is nonchondritic.

In addition to the PGE abundances, PGE ratio comparisons may yield information with regard to the possible presence of a meteoritic component. The only sample that shows anything close to a meteoritic signature is the enigmatic sample K10E from the western collar of the Vredefort Dome. This sample produces broadly chondritic Ru/Ir, Rh/Ir, and Pt/Ir ratios (within a factor of 1.5 from chondritic values), but also Pd/Ir and Au/Ir ratios significantly higher than chondritic values.

4. CONCLUSIONS

The 32 Dwyka diamictite samples from the Late Carboniferous–Early Permian Karoo Supergroup of Southern Africa, a suite of older diamictites from the Archean Witwatersrand Supergroup, and a single, enigmatic, possibly impact-derived sample of diamictite resemblance from the collar of the Vredefort Dome do not show any evidence for the presence of a meteoritic component in their PGE abundance patterns. Similarly, the siderophile element concentration patterns do not indicate any significant enrichment in the contents of Ni or Ir, compared with average crustal concentrations.

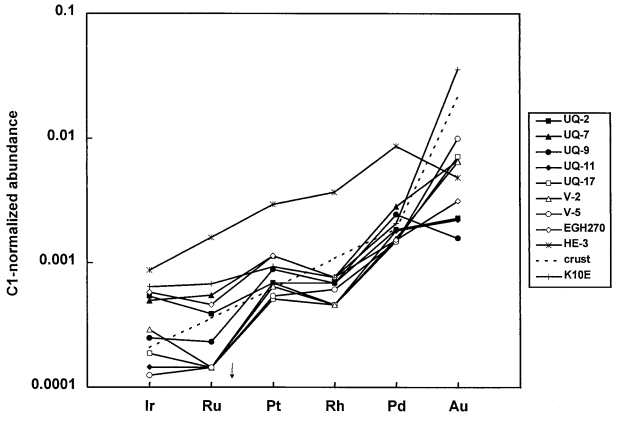

Fig. 7. C1 (Orgueil) normalization diagram of Ir, Ru, Pt, Rh, Pd, and Au of 10 diamictites. Analyses were performed by ICP-MS (see text for details). All samples show a similar trend, except HE-3 from the Government Supergroup (enriched in nearly all PGE elements). Samples that contain an extraterrestrial component would plot one or more orders of magnitude higher and have flat patterns.

All Dwyka Group and older diamictites have typically terrestrial–crustal compositions. Earlier petrographic studies of diamictites from diverse locations of the Karoo Basin (Reimold et al., 1997) and our own petrographic analysis of these sample suites failed to provide evidence for shock metamorphism. Only sample K10E from the Vredefort Dome, which even before this study was known to contain shock-metamorphosed clasts, could possibly be of impact origin, or alternatively, it could represent a shock-metamorphosed Coronation Formation diamictite. The chemical evidence provided here does not present unambiguous evidence for the presence of a meteoritic component in this sample either, although some of its PGE ratios are roughly 1.5 times chondritic.

The present investigation was carried out as a first search for geochemical evidence for an impact origin of the Dwyka Group diamictites. The results are negative in this regard and thus do not provide any support for the proposal by Oberbeck et al. (1993) and Rampino (1994) that some diamictites/tillites, specifically those investigated by us, represent impact ejecta deposits.

Acknowledgments—We are grateful to V. von Brunn for making the sampling of Dwyka diamictite in Kwa-Zulu/Natal possible. J. Visser (University of the Free State, Bloemfontein) and W. E. L. Minter (University of Cape Town, Cape Town), as well as J. Hancox (University of the Witwatersrand, Johannesburg) kindly provided additional samples for this study. GENCOR SA Limited (now part of Gold Fields of South Africa Limited) permitted sampling of the Waterpoortje drill cores and use of these materials in this study. This work was supported by the Austrian Fonds zur Förderung der wissenschaftlichen Forschung, Projekt Y-58-GEO (to C. Koeberl) and by the South African National Research Foundation (to W. U. Reimold). This is University of the Witwatersrand Impact Cratering Research Group Contribution No. 19. We appreciate helpful reviews by W. Elston and an anonymous reviewer, as well as editorial comments by H. Newsom.

Associate editor: H. E. Newsom

REFERENCES

Armstrong R. A., Compston W., Retief E. A., Williams I. S., and Welke H. J. (1991) Zircon ion microprobe studies bearing on the age and evolution of the Witwatersrand triad. Precambrian Research **53,** 243–266.

Bates R. L. and Jackson J. A. (1987) *Glossary of Geology*. American Geological Institute.

CANMET. (1994) *Catalogue of Certified Reference Materials.*CCRMP 94-1E, 82 pp.

Dressler B. O., Grieve R. A. F., and Sharpton V. L., eds. (1994) Large

meteorite impacts and planetary evolution. *Geological Society of America, Special Paper* **293,** 1–348.
Eyles C. H. and Eyles N. (1983) Glaciomarine model for upper Precambrian diamictites of the Port Akaig Formation, Scotland. *Geology* **11,** 692–694.
Flint R. F., Sanders J. E., and Rodgers J. (1960) Diamictite, a substitute term for symmictite. *Geol. Soc. Am. Bull.* **71,** 1809.
French B. M. (1998) *Traces of Catastrophe: A Handbook of Shock-Metamorphic Effects in Terrestrial Meteorite Impact Structures.* LPI Contribution 954. Lunar and Planar Institute.
Gibson R. L. and Reimold W. U. (1999) Significance of the Vredefort Dome for metamorphic-mineralization studies in the Witwatersrand Basin. *Mineral. Petrol.* **66,** 5–23.
Govindaraju K. (1989) 1989 compilation of working values and sample descriptions for 272 geostandards. *Geostand. Newsl.* **13,** 1–113.
Grieve R. A. F. (1991) Terrestrial impact: The record in the rocks. *Meteoritics* **26,** 175–194.
Grieve R. A. F., Langenhorst F., and Stöffler D. (1996) Shock metamorphism of quartz in nature and experiment: II. Significance in geoscience. *Meteoritics Planet. Sci.* **31,** 6–35.
Henkel H. and Reimold W. U. (1998) Integrated geophysical modelling of a giant, complex impact structure: Anatomy of the Vredefort Structure, South Africa. *Tectonophysics* **287,** 1–20.
Huber H., Koeberl C., McDonald I., and Reimold W. U. (2000) Use of γ-γ coincidence spectrometry in the geochemical study of diamictites from South Africa. *J. Radioanalyt. Nucl. Chem.* **244,** 603–607.
Jackson S. E., Fryer B. J., Gosse W., Healey D. C., Longerich H. P., and Strong D. F. (1990) Determination of the precious metals in geological materials by inductively coupled plasma–mass spectrometry (ICP-MS) with nickel sulphide fire-assay collection and tellurium coprecipitation. *Chem. Geol.* **83,** 119–132.
Jarosewich E., Clarke R. S. Jr., and Barrows J. N., eds. (1987) The Allende meteorite reference sample. *Smithsonian Contrib. Earth Sci.* **27,** 1–49.
Kamo S. L., Reimold W. U., Krogh T. E., and Colliston W. P. (1996) A 2.023 Ga age for the Vredefort impact event and a first report of shock metamorphosed zircons in pseudotachylitic breccias and Granophyre. *Earth Planet. Sci. Lett.* **144,** 369–388.
Koeberl C. (1993) Instrumental neutron activation analysis of geochemical and cosmochemical samples: A fast and reliable method for small sample analysis. *J. Radioanalyt. Nucl. Chem.* **168,** 47–60.
Koeberl C. (1998) Identification of meteoritic components in impactites. In: *Meteorites: Flux with Time and Impact Effects* (eds M. M. Grady, R. Hutchison, G. J. H. McCall, and D. A. Rothery), pp. 133–153. Geological Society, London, Special Publication 140.
Koeberl C., Reimold W. U., and Shirey S. B. (1996) A Re-Os isotope study of the Vredefort Granophyre: Clues to the origin of the Vredefort Structure, South Africa. *Geology* **24,** 913–916.
Koeberl C. and Huber H. (2000) Multiparameter γ-γ coincidence spectrometry for the determination of iridium in geological materials. *J. Radioanalyt. Nucl. Chem.* **244,** 655–660.
Koeberl C., Reimold W. U., McDonald I., and Rosing M. (2000) Search for petrographic and geochemical evidence for the late heavy bombardment on earth in early Archean rocks from Isua, Greenland. In: *Impacts and the Early Earth* (eds. I. Gilmour and C. Koeberl). *Lecture Notes in Earth Sciences,* Vol. 91, pp. 73–97. Springer-Verlag.
Leroux H., Reimold W. U., and Doukhan J.-C. (1994) A T.E.M. investigation of shock metamorphism in quartz from the Vredefort Dome, South Africa. *Tectonophysics* **230,** 223–239.
McDonald I. (1998) The need for a common framework for collection and interpretation of data in platinum group element geochemistry. *Geostand. Newsl.* **22,** 85–91.
Melosh H. J. (1989) *Impact Cratering: A Geologic Process*. Oxford University Press.
Montanari A. and Koeberl C. (2000) *Impact Stratigraphy: The Italian Record. Lecture Notes in Earth Sciences,*Vol. 93. Springer-Verlag.
Morgan J. W., Higuchi H., Ganapathy R., and Anders E. (1975) Meteoritic material in four terrestrial meteorite craters. In: *Proceedings of the 6th Lunar Science Conference,* pp. 1609–1623.
Oberbeck V. R., Marshall J. R., and Aggarwal H. (1993) Impacts, tillites, and the breakup of Gondwanaland. *J. Geol.* **101,** 1–19.
Palme H. (1982) Identification of projectiles of large terrestrial impact craters and some implication for the interpretation of Ir-rich Cretaceous/Tertiary boundary layers. *Geological Society of America Special Paper* **190,** 223–233.
Palme H., Janssens M.-J., Takahasi H., Anders E., and Hertogen J. (1978) Meteorite material at five large impact craters. *Geochim. Cosmochim. Acta* **42,** 313–323.
Palme H., Suess H. E., and Zeh H. D. (1981) Abundances of the elements in the solar system. In: *Landolt-Boernstein* (eds. K. Schaifers and H. H. Voigt), pp. 257–273. Springer-Verlag.
Pearson D. G. and Woodland, S. J. (1999) Solvent extraction/anion exchange separation and determination of PGEs (Os, Ir, Pt, Pd, Ru) and Re-Os isotopes in geological samples by isotope dilution ICP-MS. *Chem. Geol.* **165,** 87–107.
Rampino M. R. (1994) Tillites, diamictites, and ballistic ejecta of large impacts. *J. Geol.* **102,** 439–456.
Reimold W. U. (1995) Pseudotachylite in impact structures—Generation by friction melting and shock brecciation? A review and discussion. *Earth-Sci. Rev.* **39,** 247–264.
Reimold W. U. and Colliston W. P. (1994) Pseudotachylites of the Vredefort Dome and the surrounding Witwatersrand Basin, South Africa. In: *Large Meteorite Impacts and Planetary Evolution* (eds. B. O. Dressler, V. L. Sharpton, and R. A. F. Grieve). Geological Society of America, Special Paper **293,** 177–196.
Reimold W. U., Koeberl C., and Bishop J. (1994) Roter Kamm impact crater, Namibia: Geochemistry of basement rocks and breccias. *Geochim. Cosmochim. Acta* **58,** 2689–2710.
Reimold W. U. and Gibson R. L. (1996) Geology and evolution of the Vredefort impact structure, South Africa. *J. Afr. Earth Sci.* **23,** 125–167.
Reimold W. U., von Brunn V., and Koeberl C. (1997) Are diamictites impact ejecta? No supporting evidence from South African Dwyka Group diamictite. *J. Geol.* **105,** 517–530.
Reynolds D. K. (1991) The significance of diamictites in the Witwatersrand Government Subgroup, Klerksdorp Goldfield, South Africa. Geology Honours Project, Department of Geology, University of Cape Town, Rondebosch.
SACS (1980) The South African Committee for Stratigraphy, Stratigraphy of South Africa, Handbook 8, Kent L.E., comp., Part 1: Lithostratigraphy of the Republic of South Africa, South West Africa/Namibia and the Republics of Bophutatswana, Transkei and Venda, Gov. Printer, 690 p.
Silver L. T. and Schultz P. H., eds. (1982) Geological implications of impacts of large asteroids and comets on the Earth. *Geological Society of America, Special Paper* **190,** 1–528.
Stanistreet I. G., Martin D., Spencer R., and Beneke D. (1988) The importance of diamictites in the understanding of the tectonics and sedimentation of the Witwatersrand Basin. In: *Extended Abstracts, Geocongress 1988,* pp. 607–610. Geological Society of South Africa, Durban.
Stöffler D. (1972) Deformation and transformation of rock-forming minerals by natural and experimental shock processes. I. Behaviour of minerals under shock compression. Fortschr. Miner. **49,** 50–113.
Stöffler D. and Langenhorst F. (1994) Shock metamorphism of quartz in nature and experiment: I. Basic observation and theory. *Meteoritics* **29,** 155–181.
Taylor, S. R. and McLennan S. M., 1985. *The Continental Crust: Its Composition and Evolution.* Blackwell Scientific.
Therriault A. M., Grieve R. A. F., and Reimold W. U. (1997) The Vredefort Structure: Original size and significance for geologic evolution of the Witwatersrand Basin. *Meteoritics Planet. Sci.* **32** 71–77.
Tredoux M. and McDonald I. (1996) Komatiite Wits-1, low concentration noble metal standard for the analysis of non-mineralized samples. *Geostand. Newslett.* **20,** 267–276.
Visser J. N. J. (1994) The interpretation of massive rain-out and debris-flow diamictites from the glacial marine environment. In: *Earth's Glacial Record* (eds. M. Deynoux, J. M. G. Miller, N. Eyles, G. M. Young, E. W. Domack, and I. J. Fairchild), pp. 83–94. Cambridge University Press.
von Brunn V. (1994) Glaciogenic deposits of the Permo-Carboniferous Dwyka Group in the eastern region of the Karoo Basin, South Africa. In: *Earth's Glacial Record* (eds. M. Deynoux, J. M. G. Miller, N. Eyles, G. M. Young, E. W. Domack, and I. J. Fairchild), pp. 60–68. Cambridge University Press.